Structure of Shock Waves in Cylindrical Ducts

P. J. WALTRUP* AND F. S. BILLIG†
The Johns Hopkins University Applied Physics Laboratory, Silver Spring, Md.

Wall static and in-stream pitot pressure distributions are presented for confined, nonreacting, supersonic flows in cylindrical sections wherein a shock structure has been stabilized. Based on an analysis of these measurements, the character of the wave structure is shown to be oblique rather than normal, with the flow remaining primarily supersonic downstream of the shock system. When additional cylindrical sections are either added or deleted the shock structure is, with the exception of slight changes due to the different initial conditions, independent of location in the duct. The parameters which govern the distance s_t, over which the pressure rise is spread, viz., Mach number, momentum thickness Reynolds number, duct diameter, and the momentum thickness of the upstream boundary layer, were varied as follows: $1.53 \leqq M_a \leqq 2.72$, $5 \times 10^3 \leqq Re_\theta \leqq 6 \times 10^4$, $1.0 \leqq D \leqq 6.1$ in., and $0.007 \leqq \theta \leqq 0.036$ in. In each test the wave structure was generated by either lowering the pressure in the air supply system so that the cylindrical duct was, in effect, overexpanded when discharging to ambient conditions, or by throttling the flow leaving the duct. For a given pressure ratio across the disturbance, p_f/p_a, s_t varies approximately directly with the product $\theta^{1/2}D^{1/2}$ and inversely with $(M_a^2 - 1)Re_\theta^{1/4}$. A simple quadratic expression is presented which adequately represents this corespondence for the complete range of conditions tested and for data from the cited reference.

Nomenclature

C_f = skin-friction coefficient
D = diameter
L = length
M_a = Mach number of approach flow
p = pressure
p_t' = pitot pressure
Re_θ = Reynolds number based on boundary-layer momentum thickness
r = radius; r_d = duct radius = $D/2$
s = axial coordinate with origin at beginning of wall pressure rise
s_t = axial distance over which shock structure (or wall pressure rise) is spread
T = temperature
x = axial distance
θ = boundary-layer momentum thickness for undisturbed flow
δ^* = boundary-layer displacement thickness for undisturbed flow

Subscripts
a = initial condition
b = conditions downstream of initial shock
f = final (or duct exit) condition
r = reference conditions for normal shock at duct entrance
t_0 = total, plenum condition
w = condition at wall

Introduction

THE structure of the flow of a compressible fluid in a confined duct under the influence of a strong adverse pressure gradient has important implications in the design and operation of wind-tunnel diffusers and in the induction system in airbreathing engines. In early work Neumann and Lustwerk[1] measured wall pressure distributions in long circular ducts (L/D = 42-53) over a range of Mach numbers ($1.8 \leqq M_a \leqq 4.2$) to determine the optimum length for the design of the throat section of a wind-tunnel diffuser. When shocks were generated in the ducts the pressure rise extended over a length of 8–12 tube diameters, and efficiencies were deduced to be near that corresponding to a single normal shock. In Ref. 2 Lustwerk extended his work to testing a sharp-lipped duct in a Mach 2.05 wind tunnel in which the boundary-layer thickness at the beginning of the shock structure could be varied. He found that with no boundary-layer thickness, a normal shock is formed in a plane; as the boundary layer thickens a series of plane or lambda shocks occur and, with even further thickening, a series of oblique shocks is formed. Fejer et al.[3] studied the shock structure in rectangular ducts at M_a = 1.6–2.5 showing that various wave structures with pressure rises up nearly to the normal-shock value could be generated. Duct length/height ratios required to produce the maximum pressure rise increased from 6:1 at M_a = 1.6 to greater than 10:1 at M_a = 10. McLafferty et al., in a recently declassified report,[4] discuss shock stabilization in constant-area ducts with emphasis on application to the induction system for turbojet inlets. Test results obtained at Mach numbers of 1.76 to 2.51 showed that the interaction length increased with Mach number and decreased with initial boundary-layer displacement thickness at approximately the rate as found in Refs. 2 and 5. An analytical procedure for calculating the total pressure recovery in such a shock system is given in Ref. 6.

A similar, but not analogous, flow structure exists in the case of second-throat diffusors used in ejector systems without induced flow (see, e.g., Refs. 7–10). In this case, however, the abrupt change in geometry at the primary jet exit produces a markedly different shock structure in the duct. Finally, the flow in the more classic case of an incident shock striking the boundary-layer on an unbounded surface, e.g., a flat plate[11,12] is also not analogous because the flow external to the interaction region can readjust to compensate for the interaction.

With the advent of the supersonic combustion ramjet, "scramjet," the more general problem of shocks in ducts where the conditions downstream of the structure could be supersonic arose, whereas in all of the referenced cases the downstream condition was subsonic. In Ref. 13, results from tests of scramjet engines in hypersonic freejets and of direct-connect combustors showed that the combustion in a supersonic stream produces a shock structure in the flow upstream and that a prescribed length of "isolator" duct was required to stabilize the wave structure and prevent these combustion induced disturbances from disrupting the flow in the engine inlet. These tests and the subsequent analysis were intended to investigate this problem in a much

Received October 26, 1972; presented as Paper 72-1181 at the AIAA/SAE 8th Propulsion Joint Specialist Conference, New Orleans, La., Nov. 29–Dec. 1, 1972; revision received May 16, 1973. This work was supported by the U.S. Navy under Naval Ordnance Systems Command Contract N00017-72-C-4401.

Index categories: Nozzles and Channel Flow; Shock Waves and Detonations.

* Engineer, Hypersonic Ramjets Project. Associate Member AIAA.
† Supervisor, Hypersonic Ramjets Project. Associate Fellow AIAA.

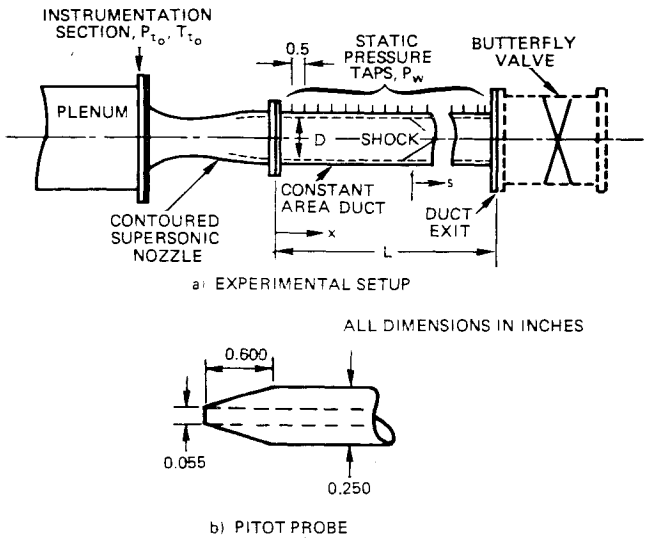

Fig. 1 Schematic of experimental apparatus.

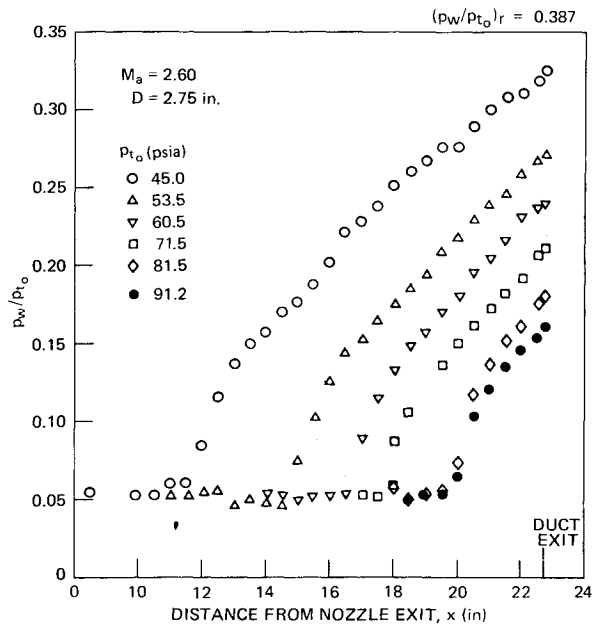

Fig. 2 Wall pressure distribution for case 3.

simpler apparatus in which the effects of combustion were simulated by either overexpansion or throttling a nonreacting flow.

Experimental Apparatus and Test Procedure

Figure 1a is a schematic of the experimental setup used in these tests which were made at the Propulsion Research Facility of The Johns Hopkins Applied Physics Lab. Compressed air (20–240 psia, ~520°R) is expanded through a contoured axisymmetric nozzle into constant-area ducts of varying length whose exits are either open to the atmosphere or throttled through a gear-driven butterfly valve. Because the supersonic nozzle usually is operated below its design stagnation pressure, the average Mach number M_a is determined by making a pitot pressure survey with a rake consisting of seven equally spaced 0.055-in.-i.d. × 0.0625-in.-o.d. steel tubes. The constant-area ducts, made of either plexiglass or steel, are instrumented with 0.015-in.-diam static pressure taps at 0.5-in. intervals. In-stream pitot surveys are made using a single steel probe (Fig. 1b) mounted on an axial traversing mechanism located downstream of the duct exit. Axial distance is measured using a precision linear potentiometer and traversing times are on the order of 6 in./min. The wall static pressures, read through a scanning valve arrangement at 1-sec intervals, and all other pressures are measured by strain-gage transducers calibrated within ±0.5% of their full-scale values.

Table 1 summarizes the conditions for each test and the method used to generate the wave structure. In cases 1–4, 7, and 8 (Table 1) the duct flow is allowed to expand to the atmosphere, and the plenum pressure p_{t_0} is reduced until a shock appears at the duct exit. From this point, p_{t_0} is lowered by steps, and $p_w(x)$ data are taken at each step, until the tunnel flow breaks down (i.e., the shock structure recedes into the air supply nozzle). To obtain data at higher Reynolds numbers, as in cases 5 and 6, p_{t_0} is held constant and a butterfly valve at the duct exit is closed by steps, taking p_w data at each, until the tunnel flow breaks down. Either procedure progressively increases the back-pressure/initial-pressure ratio p_f/p_a forcing the shock structure to recede farther into the duct and increase in strength. When in-stream pitot surveys are made (case 3), p_{t_0} is held constant at a predetermined level and axial traverses are made at five radial locations.

Experimental Results

Examples of the axial distributions of wall static pressure (p_w normalized by p_{t_0}) are shown in Figs. 2 and 3. The remainder are given in Ref. 14. In all cases the static pressure point plotted at the duct exit station p_f is the external pressure, whether it be atmospheric or that generated by throttling. The data points for the shock structures originating close to the duct exit represent the lowest value of p_f/p_a in which some definition of the shape of the pressure rise could be made (i.e., over a 1–3 in. length). The highest data points, corresponding to the highest value of p_f/p_a in which the shock structure could be stabilized in the duct, produces final wall pressures that, in all cases except for case 1 at Mach 1.53 (Ref. 14), are lower than that corresponding to a normal shock at the initial conditions $(p_w/p_{t_0})_r$. Thus, the

Table 1 Test conditions and duct configurations for shock structure experiments

Case	M_a	p_{t_0}, psia	D, in.	Duct L/D	θ, 10^3 ft	$Re_\theta \times 10^{-4}$	Normal shock conditions p_f/p_a	Normal shock conditions $(p_w/p_{t_0})_r$	Duct discharge
1	1.53	20–27	2.75	8.27	1.6 –2.15	1.07–1.85	2.56	0.669	Atm.
2	1.97	25–40	2.75	8.27	1.2 –1.95	0.86–2.15	4.36	0.584	Atm.
3	2.60	45–92	2.75	8.27	1.15–1.6	1.07–2.67	7.72	0.387	Atm.
4	2.60	45–87	2.75	6.09	0.6 –1.37	0.53–3.12	7.72	0.387	Atm.
5	2.69	195	2.75	8.27	0.8 –1.20	2.42–4.68	8.28	0.361	Throttled
6	2.72	240	2.75	8.27	0.6 –1.24	3.20–5.53	8.46	0.326	Throttled
7	2.61	50–94	6.10	8.27	2.0 –3.0	2.07–5.75	7.78	0.384	Atm.
8	1.68	29–41	1.00	8.27	0.6 –0.85	0.51–1.04	3.13	0.653	Atm.

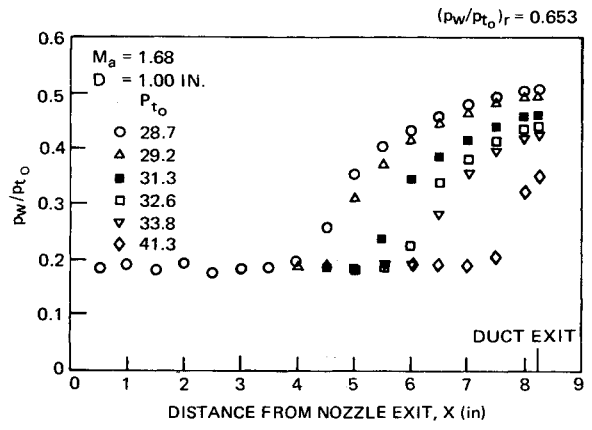

Fig. 3 Wall pressure distribution for case 8.

shock structure for at least all but one of the data points is oblique rather than normal.

A striking feature of these results is the similarity in shape and/or slope of all of the profiles for a given case. Indeed, if all profiles for any one case are shifted by matching a data point from one with the trace of another, all collapse to a single curve as shown in Fig. 4. (Cases 5, 7, and 8 are left out only for clarity.) This suggests that the wave structure for tests with p_f/p_a lower than the maximum p_f/p_a, represents just a proportional part of the wave structure present in the maximum case. To substantiate this conclusion, the pitot surveys for two points from case 3, shown in Fig. 5, were made. Since the rigidity of the in-stream probe support began to become marginal at insertion distances greater than approximately 7 in., p_f/p_a was set to levels in which the complete shock structure resided in the last 7 in. of duct length. The probe was translated at five radial locations ($r = 0$ is the duct centerline) for two values of p_f/p_a, viz., 3.22 and 4.10. Again, the pitot pressure traces also show marked similarity when plotted vs distance from the onset of the pressure rise as shown in Fig. 6, which further substantiates the arguments regarding similarity in wave structure.

Since photographic visualization of nonplanar ducted flows is nearly impossible due to diffraction of an incoming parallel light beam in the curved walls, it is necessary to reconstruct the flow from the pressure measurements to obtain some insight into the wave structure. The wave structure shown in Fig. 7 for the $p_f/p_a = 4.10$ data from Fig. 5 was constructed in the following way. From the data at $r = 0.125$ in., near the centerline, the maximum value of p_t'/p_{t_0} was used to obtain the angle of the first shock and its reflection from the centerline, i.e., p_t'/p_{t_0} corresponds to a three-shock compression system: the initial wave, its reflection, and the normal shock on the pitot tube. From the minimum value of p_t'/p_{t_0} occurring at the first node of the same

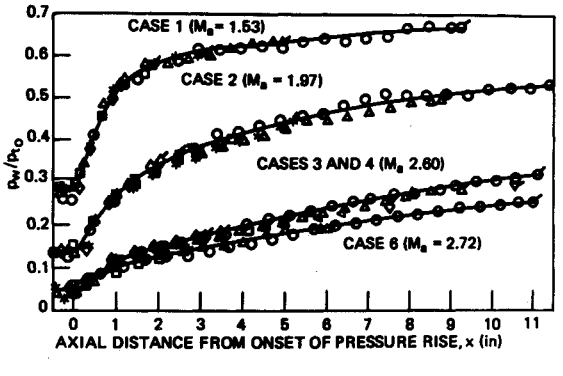

Fig. 4 Collapsed wall pressure distributions.

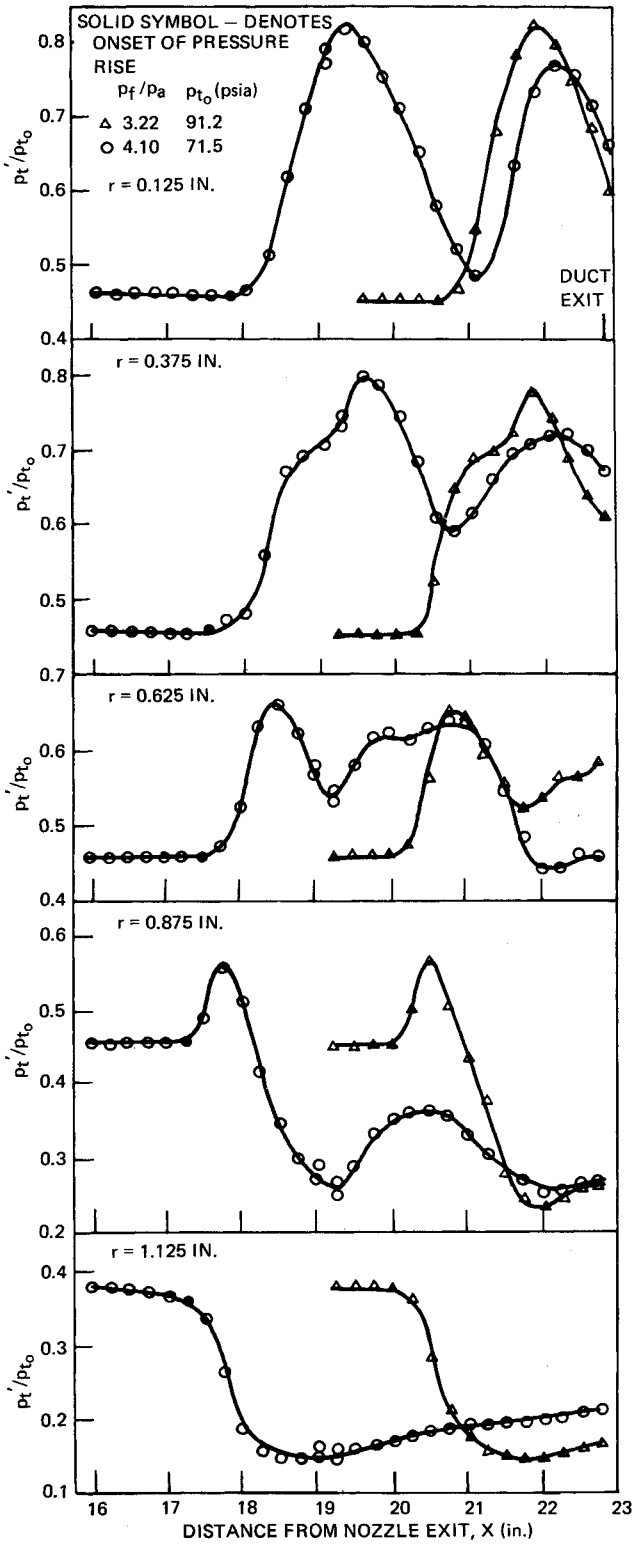

Fig. 5 Axial pitot pressure profiles for case 3.

trace the angles of the first expansion wave and its reflection from the centerline were found using a similar procedure. Here, due to the approximate nature of the analysis, expansion fans are represented by single waves and curvature of the waves is neglected except at points of intersection. The process is then repeated for the compression portion of the second cycle. The waves are then extended back to the streamline passing through δ^* at the upstream extent of the interaction region, with compatability in flow direction and pressure being observed at each wave intersection.

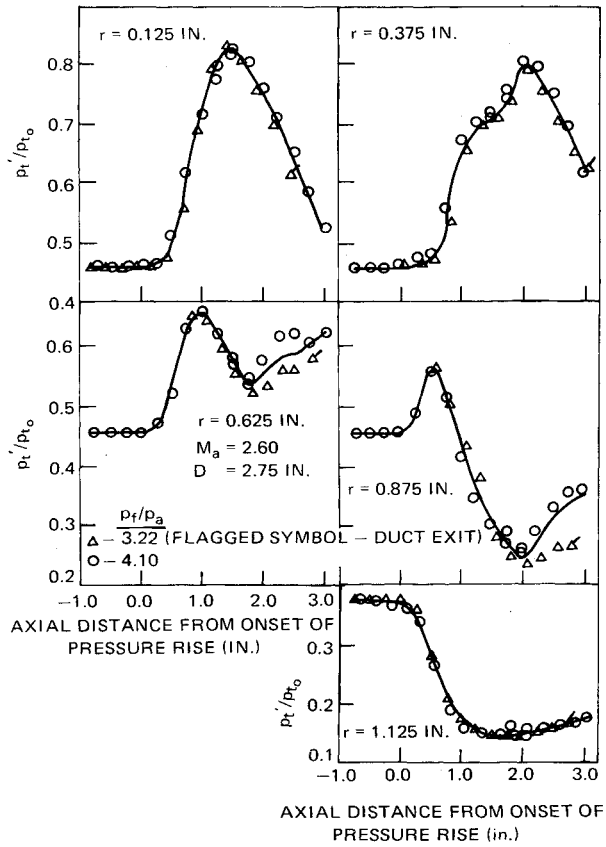

Fig. 6 Collapsed pitot pressure profiles.

Calculated local Mach numbers are shown in Fig. 7, and comparisons of the corresponding pitot pressure ratios with the measurements at $r = 0.125$ in. and $r = 0.375$ in. are given. These comparisons indicate that the general character of the shock structure has been depicted and that both the compression and expansion processes in reality consist of a multiplicity of waves

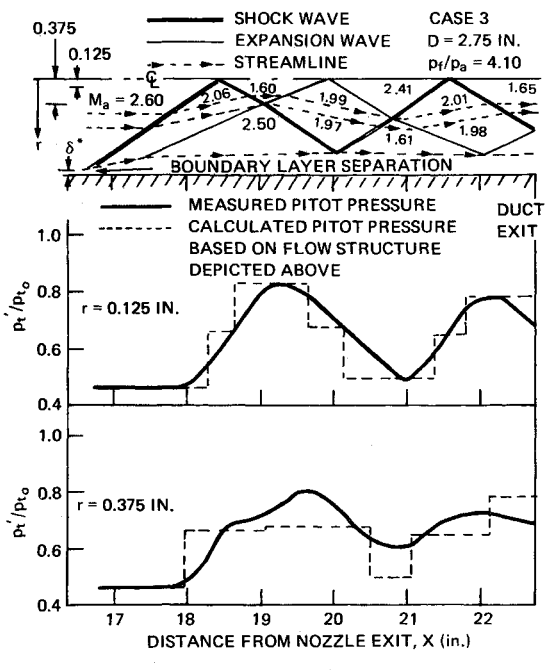

Fig. 7 Simplified representation of shock structure and comparison with pitot pressure surveys.

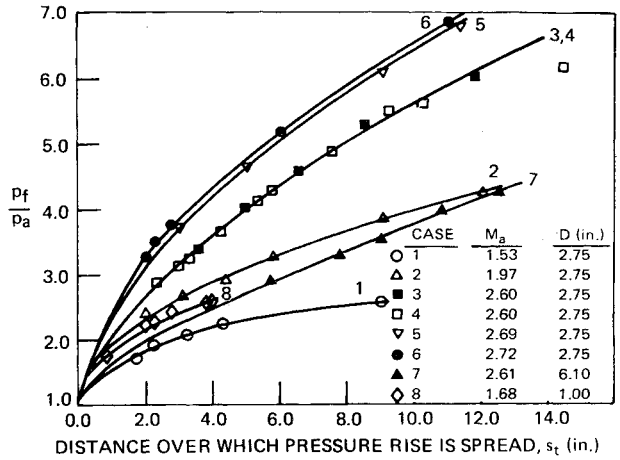

Fig. 8 Over-all pressure rise vs axial distance.

which produce continuous rather than step changes in p_t'/p_{t_0}. Note that the interaction of the probe shock with the duct wave structure also leads to a lack of precise definition of wave location. The calculated value of static pressure across the initial compression wave is 2.2, which is in general agreement with other separation criteria data.[15] Finally, the flow reconstruction coupled with the wall static pressure data shows that the flow in the duct exit is primarily supersonic for p_f/p_a values less than the corresponding normal shock value.

At this point there is a temptation to attempt to correlate all of the data on the basis of reconstructed shock structures using some appropriate separation model to obtain the initial wave angle. The inherent approximate nature of the method suggests that a more fruitful approach is to attempt to correlate the static pressure data using normalizing parameters that are consistent with the flow structure that has been postulated. When the end points p_f from each static pressure rise curve (denoted as flagged symbols in Fig. 4) are ratioed to p_a and these points are plotted vs the total distance s_t over which the pressure rise acts, the curves shown in Fig. 8 are obtained.

Since p_a/p_{t_0} is constant for each case (a given M_a) but differs for various cases, this method of plotting brings all cases to a common origin but fans them out to display the M_a effect. For a given s_t, the larger the M_a, the higher the required compression. This is just the opposite trend that would be expected if the role of boundary-layer separation was not important. That is, for a fixed pressure ratio across the initial compression wave the shock angle would decrease and the length scale would increase for larger M_a. With separation, however, the pressure ratio corresponding to separation increases with Mach number, and the shock angle increases resulting in the observed trend. A statistical analysis of the data of Fig. 8 showed that $(M_a^2-1)^{-1}$ is the simplest functional relationship which will collapse the data. Likewise, for the same p_f/p_a, s_t was found to vary inversely with $Re_\theta^{1/4}$ and directly with $D^{1/2}\theta^{1/2}$. Each of these trends is expected. The θ values for these tests were obtained from boundary-layer calculations based on the momentum-integral method of Ref. 16. As Re_θ increases, the boundary layer can withstand a larger p_b/p_a before separating, therefore the initial shock angle is steeper and s_t is smaller. The inverse scaling with diameter is due to the trend toward geometric scaling which is not strictly geometric according to the data correlation unless both D and θ change uniformly. The variation with bounday-layer thickness is in a qualitative sense the same as observed by Lustwerk[2] and in a quantitative sense consistent with that described by McLafferty in Ref. 4. Figure B-12 of that reference presents normalized s_t vs normalized δ^*. Assuming direct proportionality between θ and δ^*, it is possible to show the $\theta^{1/2}$ dependence, but considerable scatter is present in the data. In the limit, as θ approaches zero s_t should also approach zero, since it should be possible to stabilize a single,

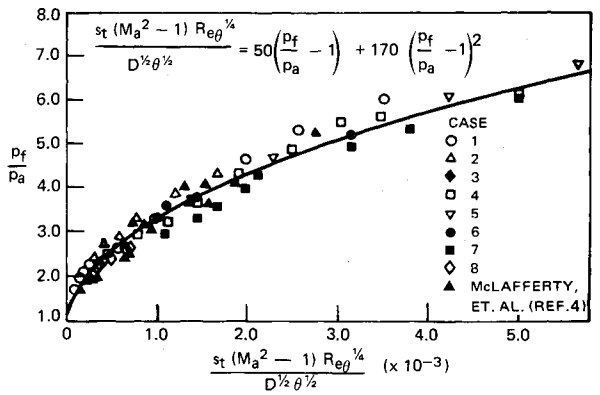

Fig. 9 Correlation of experimental data.

simple, normal shock. Just this situation was produced in a combustion experiment described in Ref. 17 in which the boundary-layer was removed just upstream of the shock.

Figure 9 shows the degree of success obtained in the correlation procedure, where the results of Ref. 4 are included in the summary. Some scatter is present but a simple quadratic relationship

$$\frac{s_t(M_a^2-1)Re_\theta^{1/4}}{D^{1/2}\theta^{1/2}} = 50\left(\frac{p_f}{p_a} - 1\right) + 170\left(\frac{p_f}{p_a} - 1\right)^2 \qquad (1)$$

as shown by the correlating curve adequately represents all of the data. The empirical correlation not only defines the end point s_t of the pressure rise curve, but the entire wall pressure distribution simply by replacing s_t with s and p_f/p_a with p_w/p_a. This is a consequence of the observation shown in Fig. 4 that, for the same initial conditions, curves for various p_f/p_a superpose when the origin of points of initial pressure rise are made to coincide. Thus p_f/p_a for a small pressure rise curve corresponds to an intermediate point on a large pressure rise curve.

Conclusions

Experimental wall pressure and instream pitot pressure distribution for shock structures in cylindrical ducts have been correlated to show the following.

1) For a given initial condition, duct diameter D, Mach number M_a, boundary-layer momentum thickness θ, and Reynolds' number Re_θ, wall pressure and pitot pressure distributions for different values of the over-all compression ratio p_f/p_a superpose.

2) For a given p_f/p_a the distance s_t, over which the pressure rise or shock structure is spread, varies inversely with $(M_a^2-1)Re_\theta^{1/4}$ and directly with $D^{1/2}\theta^{1/2}$.

3) The shock structure in the duct is governed by the conditions required to initially separate the boundary-layer in the duct. If the pressure rise corresponding to a relatively weak oblique shock is sufficient to separate the boundary-layer and the over-all duct pressure rise is greater, then a repeating, centerline-reflected shock structure is generated to produce the pressure rise. Thus, even though p_f/p_a corresponds to a normal shock at the initial conditions, the shock structure is oblique rather than normal. Although in-stream measurements were not made at low Mach numbers and/or low Reynolds numbers, presumably the shock structure would become a bifurcated, Mach-reflected shock system when the compatibility conditions for centerline reflection could no longer be met, and eventually the structure would be just a normal shock.

4) A simple quadratic relationship [Eq. (1)] can be used with the upstream flow properties to describe the wall pressure distribution in the interaction region.

References

[1] Neumann, E. P. and Lustwerk, F., "Supersonic Diffusers for Wind Tunnels," *Journal of Applied Mechanics*, June 1949, pp. 195–202.

[2] Lustwerk, F., "The Influence of Boundary Layer on the 'Normal' Shock Configuration," Meteor Rept. 61, Sept. 1950, MIT, Cambridge, Mass.

[3] Fejer, A. A. et al., "An Investigation of Constant Area Supersonic Flow Diffusion," ARL 64-81, May 1965, Aerospace Research Labs., Wright-Patterson Air Force Base, Ohio.

[4] McLafferty, G. H., Krasnoff, E. L., Ranard, E. D., Rose, W. G., and Vergara, R. D., "Investigation of Turbojet Inlet Design Parameters," Rept. R-0790-13, Dec. 1955, United Aircraft Corp., East Hartford, Conn.

[5] Wilson, R. E., "Aerodynamic Characteristics of Nozzles and Diffusers for Supersonic Wind Tunnels," Rept. DRL 281, April 1951, Univ. of Texas Defense Research Lab., Austin, Texas.

[6] McLafferty, G. H., "Theoretical Pressure Recovery Through a Normal Shock in a Duct with Initial Boundary Layer," *Journal of the Aeronautical Sciences*, Vol. 20, No. 3, March 1953, p. 169.

[7] Bauer, R. C. and German, R. C., "The Effect of Second Throat Geometry on the Performance of Ejectors Without Induced Flow," TN 61-133, Nov. 1961, ARO Inc., Arnold Engineering Development Center, Tullahoma, Tenn.

[8] German, R. C., Panesci, J. H., and Clark, H. K., "Zero Secondary Flow Ejector-Diffuser Performance Using Annular Nozzles," TDR-62-196, Jan. 1963, ARO Inc., Arnold Engineering Development Center, Tullahoma, Tenn.

[9] Panesci, J. H. and German, R. C., "An Analysis of Second-Throat Diffuser Performance for Zero-Secondary-Flow Ejector Systems," AEDC-TDR-63-249, Dec. 1963, ARO Inc., Arnold Engineering Development Center, Tullahoma, Tenn.

[10] German, R. C. and Panesci, J. H., "Improved Methods for Determining Second-Throat Diffuser Performance of Zero-Secondary-Flow Ejector Systems," AEDC-TR-65-124, July 1965, ARO Inc., Arnold Engineering Development Center, Tullahoma, Tenn.

[11] Rose, W. C., "A Method for Analyzing the Interaction of an Oblique Shock Wave with a Boundary Layer," TN D-6083, Nov. 1970, NASA.

[12] Pinckney, S. Z., "Data on Effects of Incident-Reflecting Shocks on the Turbulent Boundary Layer," TM X-1221, 1966, NASA.

[13] Billig, F. S., Dugger, G. L., and Waltrup, P. J., "Inlet-Combustor Interface Problems in Scramjet Engines," The 1st International Symposium on Air Breathing Engines, The International Airbreathing Propulsion Committee, Marseilles, France, June 1972.

[14] Waltrup, P. J. and Billig, F. S., "Precombustion Shock Structure in Scramjet Engines," AIAA Paper 72-1181, New Orleans, La., 1972.

[15] Mager, A., "On the Model of the Free, Shock-Separated, Turbulent Boundary Layer," *Journal of the Aeronautical Sciences*, Vol. 23, No. 2, Feb. 1956.

[16] Glowacki, W. J., "Fortran IV (IBM 7090) Program for the Design of Contoured Axisymmetric Nozzles for High Temperature Air," NOLTR 64-219, Feb. 1965, U.S. Naval Ordnance Lab., White Oak, Md.

[17] Billig, F. S., "Design of Supersonic Combustors Based on Pressure-Area Fields," *Eleventh Symposium (International) on Combustion*, The Combustion Inst., Pittsburgh, Pa., 1967.